EURASIAN PHYSICAL TECHNICAL JOURNAL

2024, Volume 21, No. 1 (47)

https://doi.org/10.31489/2024No1/49-56

Received: 31/01/2024 Revised: 27/02/2024 Accepted: 14/03/2024

Research Article

UDC535.37

INFLUENCE OF PLASMON EFFECT ON THE SENSITIZATION OF TITANIUM DIOXIDE BY DYE MOLECULES

Omarova G.S., Serikov T.M., Seliverstova E.V.*, Auzhanova A.A., Ibrayev N.Kh.

Institute of Molecular Nanophotonics, Karaganda Buketov University, Karaganda, Kazakhstan
**Corresponding author:* genia_sv@mail.ru

Abstract. *The influence of the plasmon effect of metal nanoparticles on electron transfer from Eosin and Rhodamine B dyes to* TiO_2 *was studied. Spectral-kinetic measurements showed that, compared to* SiO_2*, not only the intensity but also the fluorescence lifetime of both dyes decreases on the* TiO_2 *surface, which indicates the charge transfer from the dye to the semiconductor. In the presence of core@shell (Ag@*TiO_2*) plasmon nanostructures, an intensification of the fluorescence of both dyes is observed, as well as a decrease in the duration of the dyes emission. The optimal concentration for which the maximum plasmon effect was recorded is 3 wt% of Ag@*TiO_2*. The plasmon effect also leads to an increase in the efficiency of sensitization of the semiconductor by molecules of the dyes under study, which is expressed as an increase in the photovoltaic and charge-transport characteristics of the semiconductor films. The results obtained on the plasmon effect on the charge transfer process in the dye/semiconductor system can be used in the development of devices for photovoltaics, photocatalytic, and optoelectronic elements.*

Keywords: semiconductor, dye, core@shell nanostructure, plasmon effect, charge transfer, sensitization.

1. Introduction

Solar energy is one of the most widespread energy resources on our planet, which far exceeds the total needs of Earth [1]. Solar energy can be converted into electrical energy [2,3], obtain an environmentally friendly and economically profitable fuel – hydrogen, and effectively purify water resources from various pollutants [4,5]. In photovoltaic elements based on semiconductors and their sensitizers, the main processes are the absorption of light and its further transformation through photoinduced charge separation at the semiconductor/dye interface [6-9].

The process of generation and transfer of photoinduced charge carriers between dye molecules and a semiconductor plays a key role in the efficiency of photovoltaic systems [10-13]. One of the ways to increase their efficiency is to improve the absorption of light by both a semiconductor and its sensitizer, as well as creating of conditions for the effective separation of electron-hole pairs in such a system. A promising strategy for enhanced performance of photovoltaic systems is the integration of plasmon nanoparticles of metal (NPs) into the working electrode of device. This makes it possible to significantly increase the light-harvesting characteristics of the sensitizing layers [14-18] without affecting their functionality.

Metal NPs are characterized by strong interaction with incident photons through the excitation of localized surface plasmon resonance (LSPR), which can facilitate the transfer of energy and/or electrons from the NPs to both the sensitizer and the semiconductor. After the LSPR excitation, an enhanced electromagnetic field is formed around the NPs, which affects on the rate of intramolecular transitions of

.

sensitizer molecules [19,20]. Currently, a limited number of works are devoted to a comprehensive analysis of the interaction in the “dye/semiconductor/plasmonic NPs” systems. For example, the method of the model Hamiltonian was used in Ref. [21], which includes the processes of plasmon-induced energy transfer (PIRET) and charge-transfer (PICT) processes from the Au NPs to the dye molecules. It was found that PIRET deforms the dynamics of the wave packets of the excited state of the molecule. It led to the increased absorption and growth of the electron density in the LUMO orbitals of the dye molecule, which leads to a 10-fold improvement in the separation of charge carriers. A PIRET from plasmonic NPs to dye molecules was also studied in [22]. It has been shown that PIRET leads to the delayed photoluminescence in metal-conjugated fluorophores. The observed increase in the fluorescence lifetime in metal-conjugated fluorophores was confirmed by theoretical calculations. The delayed luminescence of the dye indicates a longer stay of the molecule in the excited state, which will increase the probability of electron and/or energy transfer to the semiconductor.

By the authors of [18] the electron injection kinetics from a dye into mesoporous TiO_2 layers has been studied. Multistage ultrafast electron injection in the time range of 300-400 fs was shown. The introduction of Ag NPs led to ultrafast and enhanced electron injection and a decrease in charge recombination dynamics. In this paper, the concentration dependence of the plasmon effect of Ag NPs on the sensitization process of TiO_2 semiconductor films was investigated. The influence of the core@shell ($Ag@TiO_2$) nanostructures (NSs) on various ways of the enhancement of the efficiency of charge carriers transfer and transport in the “dye/semiconductor” system is considered.

The choice of the core@shell NSs is due to the fact that often organic dyes and electrolyte is used in photovoltaic systems to regenerate dye molecules. In the electrolyte plasmonic NPs can degrade or form an oxide layer on the surface, which reduces the LSPR effect. Core@shell NSs will protect the metal NPs from oxidation by electrolyte. Also, the presence of a semiconductor shell will avoid the occurrence of recombination processes between the metal NPs and the dye.

2. Experimental part

To study the dynamics of charge transfer at the “semiconductor/dye” interface, two types of semiconductors as SiO_2 (Silufol) and TiO_2 (Sigma Aldrich) were selected, and Rhodamine B (RB) and Eosin as dyes. Semiconductor films with an area of 2 cm^2 were obtained. Next, a 1 mL of dye solution with a concentration of 10^{-4} mol/L was dropped on the surface of SiO_2 and TiO_2 films. After that, the samples were dried at room temperature for 2 hours.

To study charge transfer at the “semiconductor/dye” interface in the plasmon field $Ag@TiO_2$ NSs were synthesized, where the core is the Ag NPs and shell is TiO_2. NSs were obtained according to the method of [23]. In detail, the synthesis of $Ag@TiO_2$ NSs was carried out according to the following method. First, cores were synthesized – Ag NPs. To do this, 0.1 mmol of $AgNO_3$ (99.8%, Sigma Aldrich) is added to a solution of polyvinylpyrolidone (PVP, Sigma Aldrich) in ethylene glycol (0.5 g per 25 mL). Next, the mixture is heated with intensive stirring at 50°C for 10 minutes, after which the temperature is increased to 120°C and heated for another 30 minutes. During the reaction, the solution turned yellowish-brown, which indicates the formation of silver NPs. The obtained Ag NPs are separated from ethylene glycol by centrifugation (8000 rpm, 30 min) and washed several times sequentially with acetone and ethanol. In this way, the Ag NPs are converted to absolute ethanol, and then a TiO_2 shell is synthesized around the obtained Ag NPs. To do this, a solution of titanium tetraisopropoxide ($Ti(OCH(CH_3)_2)_4$, TIPT, Sigma Aldrich) is added to the solution of plasmonic NPs with intensive stirring. The volume ratio of TIPT and Ag NPs was equal to 1:10, respectively. The formation of titanium dioxide occurs as a result of the following chemical reaction [22]:

$$Ti(OCH(CH_3)_2)_4 + C_2H_5OH \rightarrow TiO_2 + 4(CH_3)_2CHOH$$

The resulting mixture was shaken for 24 hours on a multifunctional rotator at room temperature in the dark. The formation of a TiO_2 shell around the Ag NPs was checked both by changing the size of the metal NPs before and after the addition of TIPT using dynamic light scattering (Zetasizer Nano ZS analyzer, Malvern). Measurements showed that the average diameter of the Ag NPs were 26±7 nm (Figure 1a), and the $Ag@TiO_2$ NSs were 44±18 nm (Figure 1b). That is, the average thickness of the shell is ~9 nm. The uniformity of the coating of silver NPs with a semiconductor shell was studied using scanning electron microscopy (SEM, Mira 3LMU, Tescan). As the SEM studies have shown, the TiO_2 shell evenly covers the synthesized silver NPs. The obtained Ag@TiO_2 NSs have a spherical shape.

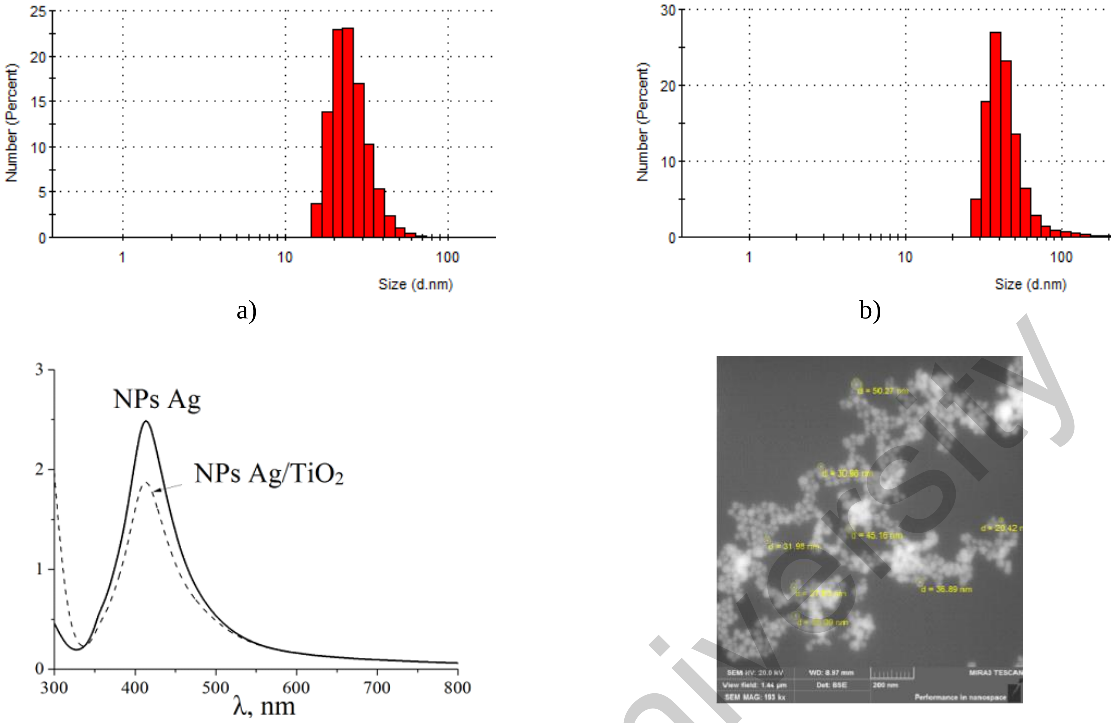

a) b)

c) d)

Fig.1. Size distribution (a, b) and absorption (c) spectrum of Ag NPs before shell synthesis (a) and NSs Ag@TiO_2 (b), as well as SEM image (d) of Ag@TiO_2 NSs

The resulting NSs were doped into the semiconductor layers. The concentration of Ag@TiO_2 NSs in TiO_2 paste was equal to 1, 2, 3 or 5 wt%. The samples obtained are designated as TCS-1 (TiO_2+core@shell, 1wt%), TCS-2, TCS-3 and TCS-5. The registration of the fluorescence lifetime of dyes in the time-correlated photon counting mode was performed with the Becker&Hickl TCSPC system. The samples were excited by a femtosecond FX200 laser (SolarLS) with λ= 515 nm and pulse duration of τ = 150 fs. The fluorescence lifetime was estimated using the SPC Image software [24] according to the procedure described in [24-26].

Dye-sensitized solar cells (DSSC) were assembled to study the effectiveness of sensitization of titanium dioxide by excited states of dyes. For this purpose, a working electrode of TiO_2 or TSC was formed on the surface of FTO-coated glasses (8 Ohms/cm^2, Sigma-Aldrich). Electrochemically deposited Pt was used as the counter electrode [27]. An iodide/triiodide electrolyte (Iodolyte Z-150, Solaronix) was used as the electrolyte. The sorption of Eosin or RB was carried out within 24 hours from an ethanol dye solution with a concentration of 10^{-4} mol/L. The DSSC was assembled according to the works of [10, 27–29]. The photovoltaic parameters of the cells were obtained from the curent-voltage characteristics recorded with solar radiation simulator CT150AAA (PET Photo Emission Tech.) at AM 1.5. The source power is 100 mW/cm^2. The charge-transport properties of the prepared films were estimated from impedance spectroscopy data in the frequency range from 1 to 100 MHz using a potentiostat/galvanostat with an integrated EIS analyzer (CS350, Corrtest Instr.). Based on the data obtained with the using of the equivalent scheme (Figure 2), the following parameters were evaluated [16, 30]: effective lifetime of charge carriers $\tau_{eff.}$, resistance to the electron transport in the material R_s(R_1) and R_k is the resistance of charge carriers' transport.

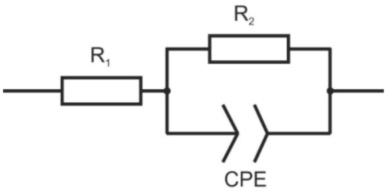

Fig.2.Equivalent electrical circuit for DSSC analysis.

3. Results and discussion

The main condition for effective sensitization of a semiconductor by dye molecules is the location of its LUMO orbital above the bottom of the TiO_2 conduction band (CB) on the energy scale. As can be seen from Figure 3, both RB and Eosin satisfy this condition. The values of HOMO/LUMO levels from the Refs. [31,32] were used to plot the diagram. The CB of SiO_2 is located higher than the LUMO level of RB or Eosin. Therefore, when the dyes are photoexcited, the charge transfer from the dyes to SiO_2 will not occur.

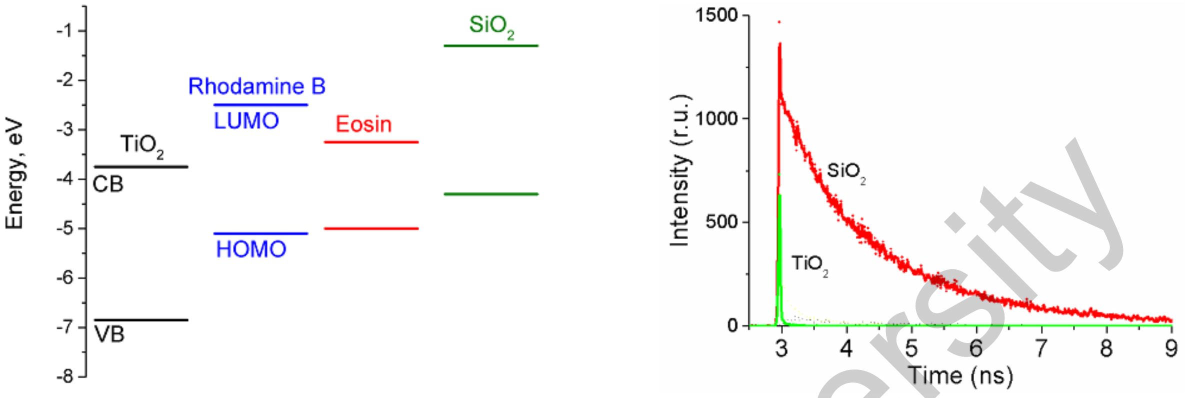

a) b)

Fig.3. (a) Energy diagram for the TiO_2 and dyes; (b) fluorescence decay kinetics of Eosin on the surface of porous SiO_2 or TiO_2 films.

In ethanol solution, the maximum of absorption band of RB exhibits at 545 nm, and the maximum of fluorescence band is at 565 nm. For Eosin, these parameters are at 525 and 545 nm.

Measurements of the spectral luminescent properties of dyes have shown that in the adsorbed state, the absorption and fluorescence spectra of RB are bathochromically shifted on the surface of SiO_2 (~20 nm compared with the dye solution in ethanol). On the surface of TiO_2, the absorption and fluorescence bands of both dyes undergo to hypsochromic shift (~5 nm compared with the dye solution in ethanol). At the same time, the fluorescence spectra of the dye are broadened.

The efficiency of charge transfer from dyes to a semiconductor was estimated from the fluorescence decay kinetics (Figure 3, Table 1). The fluorescence decay kinetics is bi-exponential. It can be seen from the data that not only the intensity, but also the lifetime of the luminescence of both dyes decreases on the surface of TiO_2. At the same time, the luminescence intensity was decreased by 1.95 times for RB, and by almost 52 times for Eosin. The average fluorescence lifetime $<\tau_{fl}>$ of RB in the presence of TiO_2 was decreased by 4.2 times. Whereas for Eosin, this ratio is equal to 7.1 times.

Table 1. Integral intensity (I) and lifetime (τ)* of fluorescence of dyes on the surface of porous SiO_2 or TiO_2 films

Sample	I (r.u.)	$<\tau_{fl}>$ (ns)	τ_1 (ns)	A_1 (%)	τ_2 (ns)	A_2 (%)
RhB						
SiO_2	128.12	1.55±0.01	0.950±0.01	59.0	2.30±0.01	41
TiO_2	65.65	0.37±0.01	0.156±0.01	79.0	0.99±0.01	21
Eosin						
SiO_2	1705.04	1.49±0.01	0.995±0.01	54.3	2.09±0.01	45.7
TiO_2	32.88	0.21±0.01	0.130±0.01	81.0	0.556±0.01	19.0

*$<\tau_{fl}>$ – average lifetime of fluorescence estimated form the equation $\langle \tau_{fl} \rangle = \sum_{i=1}^{n} A_i \tau_i$, where τ_i is the lifetime of the i-th component of fluorescence decay, A_i is the magnitude (the part of contribution) of i-th component of fluorescence decay ($\sum_i A_i$ =1,0).

The observed quenching of the fluorescence lifetime indicates the electron transfer from an excited dye molecule to a semiconductor [31]. In the case of Eosin, charge transfer from the dye to the semiconductor is carried out more efficiently.

A pure TiO_2 film, which was not sensitized with a dye, demonstrates a low-intensity signal associated with scattered radiation. The lifetime of such signal is ~10 ps, which is associated with the instrumental response function (IRF) of the measuring system. Since the wavelength of the exciting laser does not coincide in position with the absorption of TiO_2, the recorded signal can be considered as a background signal. When the Eosin and Rhodamine were adsorbed into TiO_2 films without plasmon NSs, the duration of the recorded signal from the dye was on an order of magnitude longer.

Measurements showed that in the presence of plasmon NSs, an intensification of fast fluorescence of both RB and Eosin is observed (Table 2). Changes in the fluorescence intensity of the dye registered at various concentration of core@shell NSs have a nonlinear character with a maximum at 3 wt% for RB and Eosin. At the same concentrations, the maximum reduction in the fluorescence lifetime of the dye is observed. A further increase in the content of plasmonic NSs in the film leads to a decrease in the intensity enhancement of the dyes and the restoration of the luminescence lifetimes to its original value.

Table 2. Effect of $Ag@TiO_2$NSs concentration in TiO_2 film on the intensity (I) and average fluorescence lifetime ($<\tau_{fl}>$) of dyes.

Core@shell concentration(wt%)	I (r.u.)	I_{TCS}/I_0	$<\tau_{fl}>$ (ns)	$<\tau_{fl\ TCS}>/<\tau_{fl}>$
RB				
TiO_2 neat	12.2	–	0.01	–
TiO_2	65.7	–	0.370±0.01	–
TCS-1	250.3	3.8	0.367±0.01	0.99
TCS-2	281.6	4.3	0.323±0.01	0.87
TCS-3	329.3	5.0	0.299±0.01	0.80
TCS-5	321.1	4.9	0.327±0.01	0.88
Eosin				
TiO_2 neat	12.2	–	0.01	–
TiO_2	32.89	–	0.210±0.01	–
TCS-1	86.7	2.6	0.205±0.01	0.98
TCS-2	124.7	3.8	0.200±0.01	0.95
TCS-3	136.7	4.2	0.190±0.01	0.90
TCS-5	131.2	4.0	0.207±0.01	0.99

The observed increase in the fluorescence intensity of dyes is associated with a plasmon enhancement of the radiative rate of fluorophore molecules in the near field of plasmon NPs, as shown in Ref. [25,33]. The decrease in fluorescence enhancement may be result of two factors. The first of them relates to the quenching of the fluorophore by plasmon NPs through the Förster energy transfer [25,33]. The second channel can be associated with a plasmon enhancement of the quenching of dye molecules by electron transfer to the CB of a semiconductor.

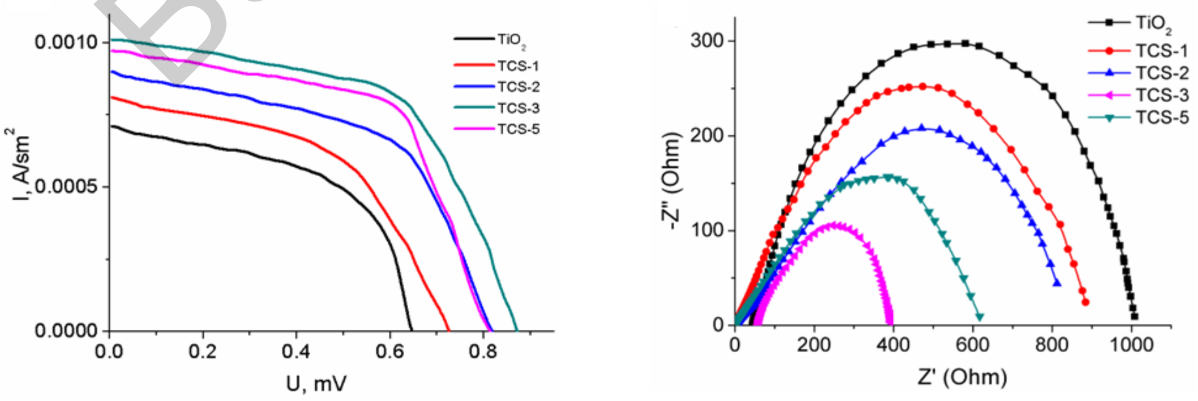

a) b)

Fig.4.The effect of the concentration of the core@shell NSs on the CVC (a) and impedance spectra (b) of DSSCs sensitized by Eosin.

.

To detail these channels, the photovoltaic and charge-transport properties of DSSCs with the addition of plasmon NSs sensitized by RB or Eosin were estimated. In the absence of plasmon NSs in the TiO_2 film, the current density, which is directly related to the number of photogenerated charge carriers in the working electrode, is equal to 0.0007 A/cm^2 and 0.00088 A/cm^2 for Eosin and Rhodamine B, respectively (Figure4, Table 3).

Table 3. Effect of the concentration of Ag@TiO_2 NSs in the TiO_2 film on the photovoltaic and charge-transport parameters of DSSCs sensitized by RB or Eosin.

Sample	U_{oc} (mV)	J_{sc} (A/cm^2)	Efficiency (%)	R_s(Ohm)	R_p(Ohm)	τ_{eff}(s)
RB						
TiO_2	64.00	0.00088	0.0047	15.00	1000	0.36
TCS-1	71.00	0.00089	0.0068	18.00	820	0.27
TCS-2	72.00	0.00100	0.0072	21.00	580	0.24
TCS-3	77.00	0.00110	0.014	23.00	190	0.22
TCS-5	80.00	0.00109	0.0074	26.00	250	0.26
Eosin						
TiO_2	65.00	0.00070	0.0010	25.00	1008	0.32
TCS-1	72.00	0.00080	0.0018	13.00	900	0.24
TCS-2+ Eosin	81.00	0.00090	0.0027	12.00	810	0.22
TCS-3+ Eosin	87.00	0.00098	0.025	35.00	400	0.18
TCS-5+ Eosin	82.00	0.00110	0.021	8.00	600	0.22

The addition of Ag@TiO_2 NSs leads to an increase in the values of the short-circuit current density. This is reflected in the increased efficiency of DSSCs. The maximum increase in the efficiency of solar cells was recorded at an Ag/TiO_2 concentration equal to 3 wt% for both dyes. Impedance measurements and estimation of electrophysical parameters have shown that the resistance and effective lifetime of charge carriers τ_{eff} in the TiO_2 film decreases under the influence of the plasmon effect of Ag NSs. Thus, the R_s resistance of TCS-3+dye films are almost in 2.5 times and 5 times less for Eosin and RB, respectively, than in TiO_2+dye samples. The resistance to electronic transport of films decreased from 1008 to 400 Ohms for Eosin and from 1000 to 190 Ohms for Rhodamine.

Thus, it can be seen that the addition of core@shell NSs to the volume of the semiconductor leads to a reduction in the lifetime of charge carriers in the semiconductor, preventing their recombination. This is reflected in an increase in the efficiency of electron migration and counting from the semiconductor surface, leading to an increase in the photocurrent density and an increase in efficiency of DSSCs.

4. Conclusions

The plasmon effect of metal nanoparticles on electron transfer to TiO_2 from Eosin and RB dyes has been studied. Spectral-kinetic measurements have shown that, compared with SiO_2, not only the intensity but also the duration of fluorescence of both dyes decreases on the surface of TiO_2. At the same time, in the case of Eosin, charge transfer from the dye to the semiconductor is carried out more efficiently. In the presence of plasmonic NSs, an intensification of fast fluorescence of both dyes is observed, as well as a decreasing in the luminescence lifetimes. The optimal concentration for which the maximum plasmon effect was recorded is equal to 3 wt% of Ag/TiO_2 NSs. The observed increase in the intensity and decrease in the fluorescence lifetimes of dyes is associated with a plasmonic enhancement in the radiative rate in dyes molecules in the near field of plasmonic NSs. Measurements of electrophysical parameters have shown that the plasmon effect also leads to an increase in the efficiency of semiconductor sensitization by molecules of the studied dyes, which is expressed in an increase in the photovoltaic and charge-transport characteristics of the studied semiconductor films. Detailed establishment of the ways of exposure of plasmonic NPs on various ways of sensitization enhancement of the TiO_2 by dye molecules will be studied in our further research.

Conflict of interest statement

The authors declare that they have no conflict of interest in relation to this research, whether financial, personal, authorship or otherwise, that could affect the research and its results presented in this paper.

CRediT author statement:
Omarova G.S.: investigation, data curation; Serikov T.M.: methodology, investigation, formal analysis, writing - original draft; Seliverstova E.V.: validation, formal analysis, writing - original draft, writing - review & editing; Auzhanova A.A.: investigation; Ibrayev N.Kh.: conceptualization, writing - original draft, writing - review & editing.
The final manuscript was read and approved by all authors.

Funding

This research is funded by the Science Committee of the Ministry of Science and Higher Education of the Republic of Kazakhstan (Grant No. AP19680241).

References

1 Pourasl H.H., Barenji R.V., Khojastehnezhad V.M. Solar energy status in the world: A comprehensive review. *Energy Reports*, 2023, Vol. 10, pp. 3474 – 3493. https://doi.org/10.1016/j.egyr.2023.10.022

2 Chiarello G.L., Dozzi M.V., Selli E. TiO_2–based materials for photocatalytic hydrogen production. *Journal of Energy Chemistry*. 2017, Vol. 26(2), pp. 250–258. https://doi.org/10.1016/j.jechem.2017.02.005

3 Ibrayev N., Seliverstova E., Aimukhanov A., Serikov T. Role of energy transfer in conversion of light to electric energy. *Molecular Crystals and Liquid Crystals*. 2014, Vol. 589, pp. 202 – 208. https://doi.org/10.1080/15421406.2013.872827

4 Sun X.Y., Wang C.Y., Su D.W., Wang G., Yunhao Z. Application of photocatalytic materials in sensors. *Advanced Materials Technologies*, 2020, Vol. 5, pp.1900993. https://doi.org/10.1002/admt.201900993

5 Tong H, Ouyang S.X., Bi Y.P., Umezawa N., Oshikiri M., Ye J. Nano-photocatalytic materials: possibilities and challenges. *Advanced Materials*. 2012, Vol. 24, pp. 229 – 251. https://doi.org/10.1002/adma.201102752

6 Clifford J.N., Martínez–Ferrero E., Viterisi A., Palomares E. Sensitizer molecular structure–device efficiency relationship in dye sensitized solar cells. *Chemical Society Reviews*. 2011, Vol. 40(3), pp. 1635 – 1646. https://doi.org/10.1039/B920664G

7 Ardo S., Meyer G.J. Photo-driven heterogeneous charge transfer with transition–metal compounds anchored to TiO_2 semiconductor surfaces. *Chemical Society Reviews*. 2009, Vol. 38(1), pp. 115-164.
https://doi.org/10.1039/B804321N

8 Haque S.A., Palomares E., Cho B.M., Green A. N. M., Hirata N., Klug D. R., Durrant, J. R. Charge separation versus recombination in dye–sensitized nanocrystalline solar cells: the minimization of kinetic redundancy. *Journal of the American Chemical Society*. 2005, Vol. 127(10), pp. 3456 – 3462. https://doi.org/10.1021/ja0460357

9 Anderson N.A., Lian T.Q. Ultrafast electron transfer at the molecule–semiconductor nanoparticle interface. *Annual Review of Physical Chemistry*. 2005, Vol. 56(1), pp. 491–519. https://doi.org/10.1146/annurev.physchem.55.091602.094347

10 Regan B.O., Grätzel M. A low-cost, high-efficiency solar cell based on dye sensitized colloidal TiO_2 films. *Nature*. 1991, Vol. 353(6346), pp. 737 – 740. https://doi.org/10.1038/353737a0

11 Hagfeldt A., Boschloo G., Sun L., Kloo L., Pettersson H. Dye-sensitized solar cells. *Chemical Reviews*, 2010, Vol. 110(11), pp.6595 – 6663. https://doi.org/10.1021/cr900356p

12 Listorti A., O'Regan B., Durrant J. R. Electron transfer dynamics in dye sensitized solar cells. *Chemistry of Materials*. 2011, Vol. 23, pp. 3381. https://doi.org/10.1021/cm200651e

13 Wang J., Liu K., Ma L., Zhan X. Triarylamine: Versatile platform for organic, dye-sensitized, and perovskite solar cells. *Chemical Reviews*. 2016, Vol. 116(23), pp. 14675 – 14725. https://doi.org/10.1021/acs.chemrev.6b00432

14 Zhou N., López-Puente V., Wang Q., Polavarapu L., Pastoriza-Santos I., Xu Q.-H. Plasmon-enhanced light harvesting: applications in enhanced photocatalysis, photodynamic therapy and photovoltaics. *RSC Advances*. 2015, Vol. 5, pp. 29076-29097. https://doi.org/10.1039/C5RA01819F

15 Adnan A., Fedwa E., Anirban M., Brahim A. Research progress of plasmonic nanostructure-enhanced photovoltaic solar cells. *Nanomaterials*. 2022, Vol. 12(5), pp. 788. https://doi.org/10.3390/nano12050788

16 Ibrayev N., Omarova G., Seliverstova E., Ishchenko A., Nuraje N. Plasmonic effect of Ag nanoparticles on polymethine dyes sensitized titanium dioxide. *Engineered Science*. 2021, Vol. 14, pp. 69 – 77. https://doi.org/10.30919/es8d1168

17 Jiang N., Zhuo X., Wang J. Active plasmonics: principles, structures and applications. *Chemical Reviews*, 2018, Vol. 118(6), pp. 3054 – 3099. https://doi.org/10.1021/acs.chemrev.7b00252

18 Biswas C, Ahmed S., Santosh S., Kumar R.S.S. Ultrafast electron injection kinetics and effect of plasmonic silver nanoparticle at organic dye-TiO_2 interface. *Asian Journal of Physics*. 2021, Vol. 30(6), pp. 933 – 945. https://doi.org/10.54955/AJP.30.6.2021.933-945

19 Geddes C.D., Lakowicz J.R. Metal–enhanced fluorescence. *Journal of Fluorescence*, 2002, Vol. 12, pp. 121 – 129. https://doi.org/10.1023/A:1016875709579

.

20 Maier S.A. *Plasmonics fundamentals and applications*. NY, Springer, 2007, 209p. https://doi.org/10.1007/0-387-37825-1

21 Zhang B., Zhao Y., Liang W. Collaborative effect of plasmon-induced resonance energy and electron transfer on the interfacial electron injection dynamics of dye-sensitized solar cell. *The Journal of Chemical Physics*.2019, Vol.151(4), pp. 044702. https://doi.org/10.1063/1.5111601

22 Yang M., Moroz P., Jin Z., Budkina D. S., Sundrani N., Porotnikov D., Zamkov M. Delayed photoluminescence in metal-conjugated fluorophores. *Journal of the American Chemical Society*, 2019, Vol. 141(28), pp. 11286 – 11297. https://doi.org/10.1021/jacs.9b04697

23 Afanasyev D.A., Ibrayev N.Kh., Serikov T.M., Zeinidenov A.K. Effect of the titanium dioxide shell on the plasmon properties of silver nanoparticles. *Russian Journal of Physical Chemistry A*. 2016, Vol. 90(4), pp. 833 – 837. https://doi.org/10.1134/S0036024416040026

24 Becker W. *The BH TCSPC e-Handbook*, 2023. https://www.becker-hickl.com/literature/documents/flim/the-bh-tcspc-handbook

25 Ibrayev N.Kh., Seliverstova E. V., Valiev R. R., Kanapina A. E., Ishchenko A. A., Kulinich A. V., Kurten T., Sundholm D. Influence of plasmons on the luminescence properties of solvatochromicmerocyanine dyes with different solvatochromism. *Physical Chemistry Chemical Physics*. 2023, Vol. 25, pp. 22851 – 22861. https://doi.org/10.1039/D3CP03029F

26 Kanapina A.E., Seliverstova E.V., Ibrayev N.K., Derevyanko N.A., Ishchenko A.A. Features of the decay of excited states of ionic dyes in the near field of metal nanoparticles. *Eurasian Physical Technical Journal*. 2023, Vol. 20, No. 2(44), pp. 106 – 111. https://doi.org/10.31489/2023NO2/106-111

27 Ibrayev N.Kh., Seliverstova E.V., Omarova G.S., Derevyanko N.A., Khamza T., Photovoltaic properties of functionalized indodicarbocyanine dye. *Eurasian Physical Technical Journal*, 2022, Vol. 19(3), pp. 55–59. https://doi.org/10.31489/2022No3/55-59

28 Ito S., Murakami T.N., Comte P., Liska P., Grätzel C., Nazeeruddin M.K., Grätzel M. Fabrication of thin film dye sensitized solar cells with solar to electric power conversion efficiency over 10%. *Thin Solid Films*, 2008, Vol.516(14), pp. 4613 – 4619. https://doi.org/10.1016/j.tsf.2007.05.090

29 Yang C.C., Zhang H., Zheng Y. DSSC with a novel Pt counter electrodes using pulsed electroplating techniques. *Current Applied Physic*. 2011, Vol. 11, pp. S147-S153. https://doi.org/10.1016/j.cap.2010.11.012

30 Bisquert J., Garcia-Belmonte G., Fabregat-Santiago F., Bueno P.R. Theoretical models for ac impedance of finite diffusion layers exhibiting low frequency dispersion. *Journal of Electroanalytical Chemistry*. 1999, Vol. 475, pp.152 – 63. https://doi.org/10.1016/S0022-0728(99)00346-0

31 Zhang F., Shi F., Ma W., Gao F., Jiao Ya. Controlling adsorption structure of Eosin Y dye on nanocrystalline TiO_2 films for improved photovoltaic performances. *The Journal of Physical Chemistry C*, 2013, Vol. 117. pp. 14659 – 14666. https://doi.org/10.1021/jp404439p

32 Kim H., Do–Hyun L., Son Y. Electrochemical study on Rhodamine 6G–indole, based dye for HOMO and LUMO energy levels. *Textile Coloration and Finishing*. 2013, Vol.25(1), pp. 83 – 88. https://doi.org/10.5764/TCF.2013.25.1.7

33 Seliverstova E., Ibrayev N., Omarova G., Ishchenko A., Kucherenko M. Competitive influence of the plasmon effect and energy transfer between chromophores and Ag nanoparticles on the fluorescent properties of indopolycarbocyanine dyes. *Journal of Luminescence*. 2021, Vol. 235, p. 118000. https://doi.org/10.1016/j.jlumin.2021.118000

AUTHORS' INFORMATION

Ibrayev, N.Kh. – Doctor of Phys. and Math. Sciences, Professor, Director of the Institute of Molecular Nanophotonics, E.A. Buketov Karaganda University, Karaganda, Kazakhstan; ORCID iD: 0000-0002-5156-5015; niazibrayev@mail.ru

Omarova, G.S.– PhD, Associate Professor, E.A. Buketov Karaganda University, Karaganda, Kazakhstan; ORCID iD: 0000-0003-2900-2168;guldenserikovna@mail.ru

Serikov, T.M. – PhD, Associate Professor, E.A. Buketov Karaganda University, Karaganda, Kazakhstan; ORCID iD: 0000-0003-4302-96744; serikov-timur@mail.ru

Seliverstova, E.V. – PhD (Phys.), Senior Research Fellow, Institute of Molecular Nanophotonics, E.A. Buketov Karaganda University, Karaganda, Kazakhstan; ORCID iD: 0000-0002-9507-8825; genia_sv@mail.ru

Auzhanova, A.A.– Master student, E.A. Buketov Karaganda University, Karaganda, Kazakhstan; ORCID iD: 0009-0002-3963-6367; aliya26122001@gmail.com